Contents lists available at SciVerse ScienceDirect

Thin Solid Films

journal homepage: www.elsevier.com/locate/tsf

Investigation of germanium implanted with aluminum by multi-laser micro-Raman spectroscopy

A. Sanson [a],*, E. Napolitani [b], G. Impellizzeri [c], M. Giarola [d], D. De Salvador [a], V. Privitera [c], F. Priolo [c], G. Mariotto [d], A. Carnera [a]

[a] Dipartimento di Fisica e Astronomia, Università di Padova, Via Marzolo 8, I-35131 Padova, Italy
[b] MATIS IMM-CNR at Dipartimento di Fisica e Astronomia, Università di Padova, Via Marzolo 8, I-35131 Padova, Italy
[c] MATIS IMM-CNR and Dipartimento di Fisica e Astronomia, Università di Catania, Via S. Sofia 64, I-95123 Catania, Italy
[d] Dipartimento di Informatica, Università di Verona, Strada le Grazie 15, I-37134 Verona, Italy

ARTICLE INFO

ABSTRACT

Germanium samples, implanted with aluminum and annealed, have been investigated by micro-Raman spectroscopy using different excitation lines with the aim of gaining insights about the Al distribution at different depths beneath the sample surface and to correlate the Raman spectra with the electrical and chemical profiles, obtained by Spreading Resistance Profiling (SRP) and Secondary Ions Mass Spectrometry (SIMS) measurements, respectively. The intensity of the Al–Ge Raman peak at about 370 cm^{-1}, due to the local vibrational mode of the substitutional Al atoms in the Ge matrix, has been directly related to the SRP behavior, while no correlation has been observed with SIMS profiles. These findings show that the electrically active content is entirely due to the substitutional Al atoms. Finally, a clear down shift is observed for the Ge–Ge Raman peak at ~300 cm^{-1}, which also seems to be directly related to the active content of Al dopant atoms. This work shows that micro-Raman spectroscopy can be a suitable tool for the study of doping profiles in Ge.

1. Introduction

In the last decade, germanium has received renewed interest as a substitute of silicon for microelectronic applications, due to its higher carrier mobility and lower band gap compared to silicon, together with the advantage of being compatible with existing Si processing technologies [1–4]. Compared to the diffusion and doping processes in Si, which have been studied extensively over more than 40 years, similar comprehensive studies in Ge, demanded for the integration of Ge-based electrical junctions in the future electronic devices, are still lacking.

Among p-type dopants in Ge [5,6], Al is a suitable choice thanks to its high solid solubility, i.e., $4.3 \cdot 10^{20}$ cm^{-3} at 675 °C as given in ref. [7]. However, only few studies concerning Al are reported in the literature [8–10]. In our recent work [10], Secondary Ions Mass Spectrometry (SIMS) and Spreading Resistance Profiling (SRP) measurements showed that, below 700 °C, Al does not diffuse and a remarkable electrical activation of about 1×10^{20} cm^{-3} is obtained (Fig. 1). Differently, at higher annealing temperatures, Al shows a significant diffusion towards the bulk and an unexpected uphill diffusion near the surface, where the electrical measurements indicate a significant deactivation of Al. Although these experimental results were tentatively explained in

terms of the presence of dopant traps, able to make immobile and electrically inactive the dopant ions nearby to the surface [10], many aspects of Al diffusion and activation are still unclear. For this reason, additional investigations are required.

In this work, a micro-Raman spectroscopy investigation was carried out on Ge samples implanted with Al and annealed at 400 °C and 400 °C + 700 °C (corresponding to high and low contents of electrically active Al, respectively). By means of the use of different excitation laser lines, which allow to probe different optical penetration depths (see below), the Al-implanted Ge samples were studied at different depths far from the sample surface. This allows us to gain insights on the Al distribution at different depths beneath the sample surface and to correlate the Raman spectra with the electrical and chemical profiles, provided by SRP and SIMS measurements, respectively.

2. Experimental details

Ge samples implanted with Al were prepared on Ge Czochralski wafers, n-type Sb-doped with (100) orientation and resistivity >40 Ω cm. Al ions were implanted with an energy of 25 keV and a dose of 1.0×10^{15} Al/cm^2. The samples were annealed at 400 °C for 1 h to induce the recrystallization of the Ge matrix by solid-phase epitaxy. Afterwards, the second sample was annealed for 1 h at 700 °C. At this temperature, a strong electrical deactivation is observed (Fig. 1). Chemical depth profiles of Al were obtained by

* Corresponding author.
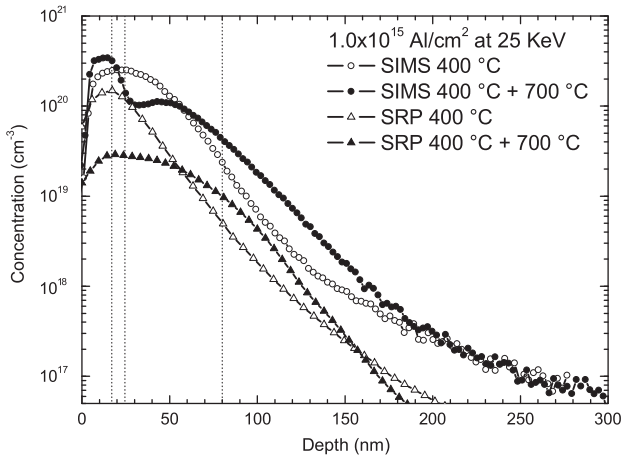 E-mail address: andrea.sanson@unipd.it (A. Sanson).

Fig. 1. SRP and SIMS profiles (circles and triangles, respectively) in samples annealed at 400 °C (open symbols) and 400 °C + 700 °C (full symbols). The vertical dotted-lines indicate (from left to right) the optical absorption length in germanium for laser lines 514.5 nm, 568.2 nm and 647.1 nm, respectively. The values were taken from Ref. [13].

secondary ion mass spectrometry (SIMS), using a Cameca IMS-4f instrument, by collecting Al$^+$ secondary ions while sputtering with a 3 keV O$_2^+$ analyzing beam. Spreading Resistance Profiling (SRP) measurements were taken on beveled sample surfaces using an SSM 150 system running at 5 g. More details on the sample preparation, SIMS and SRP characterization can be found in Ref. [10].

Polarized micro-Raman spectra were collected at room temperature in backscattering geometry using a triple monochromator (Horiba-Jobin Yvon, model T64000), equipped with holographic gratings having 1800 lines/mm and set in double-subtractive/single configuration. The spectra were excited by the 514.5 nm, 568.2 and 647.1 nm line of a mixed Ar–Kr ion gas laser focused onto a spot of 2 μm in size through the lens of a 100× microscope objective (N.A. = 0.90). The laser power on the sample surface was kept between 5 and 15 mW (depending on the laser line) to avoid thermal heating. To maximize the intensity of both Ge–Ge and Al–Ge Raman peaks, the Raman measurements were performed in crossed XY polarization orienting the samples at $\theta = 0°$ (see below). For each sample and laser line, at least three spectra have been collected at different positions on the sample surface. The scattered radiation, filtered by the fore double monochromator, was detected at the spectrograph output by a charge-coupled-device detector, cooled by liquid nitrogen, with 1024 × 256 pixels and spectral resolution better than 0.6 cm^{-1}/pixel.

3. Results and discussion

Raman spectroscopy is a suitable technique for probing both the micro-structure and the vibrational dynamics of single crystals, namely semiconductors, and in the case of an ideal Ge crystal, with space group O_h7 ($Fd3m$), the usual selection rule for the wave-vector $\mathbf{q} = 0$ accounts for a single, narrow Raman peak, with a Lorentzian shape of symmetry F_{2g}. Lattice distortions induced by impurity atoms, either interstitial or substitutional, incorporated into the crystalline matrix, lead to a relaxation of this selection rule, with relevant spectral effects like peak broadening, asymmetry and peak wave-number shift or the occurrence of new peaks due to Raman active local vibrational modes.

The Raman spectra, measured with the three different excitation laser lines, are displayed in Fig. 2: solid and dashed lines refer to the samples annealed at 400 °C and 400 °C + 700 °C, respectively; dotted lines refer to the pure Ge Czochralski wafer here used as reference. The spectra exhibit an intense band at about 300 cm^{-1}, which corresponds to the expected transverse optical phonon-mode of germanium
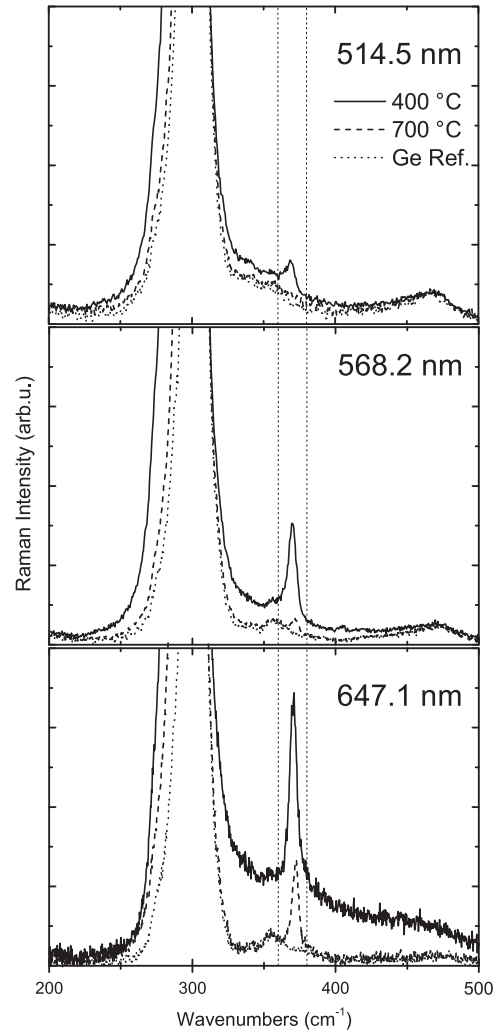

Fig. 2. Raman spectra observed with different excitation lines (i.e., 514.5 nm, 568.2 nm and 647.1 nm) in samples annealed at 400 °C and 400 °C + 700 °C (solid and dashed lines, respectively). Dotted lines are the Raman spectra of pure germanium here reported for comparison. The vertical scale is enlarged to show the Al–Ge Raman peak at ~370 cm^{-1}.

with F_{2g} symmetry. More importantly, a weak peak is observed at about 370 cm^{-1}. This peak can be attributed to the local vibrational mode of the substitutional Al atoms in the Ge matrix for the following reasons:

i) According to Contreras et al. [11], the frequency of the vibrational local mode of a substitutional atom can be estimated using the simplified mass-defect secular equation [12] that, in the case of the substitutional Al atoms in Ge, gives

$$\nu_{Al-Ge} = \nu_{Ge-Ge}\sqrt{\frac{0.35 + 0.65\, m_{Al}/m_{Ge}}{m_{Al}/m_{Ge}}} \simeq 379\, cm^{-1} \tag{1}$$

where $m_{Al}/m_{Ge} \simeq 0.37$ and $\nu_{Ge-Ge} \simeq 300$ cm^{-1}. Taking into account that this model assumes that the force constants are the same for the Al–Ge and Ge–Ge pairs, our experimental frequency (~370 cm^{-1}) is very close to the predicted frequency (~379 cm^{-1}) thus supporting our statement;

ii) The Raman scattering tensor of the Ge–Ge mode at ~300 cm^{-1} is

$$\alpha\left(F_{2g}\right) = \begin{pmatrix} 0 & a & a \\ a & 0 & a \\ a & a & 0 \end{pmatrix} \tag{2}$$

therefore the intensity of the Raman Ge–Ge peak, in back-scattering geometry, changes as $\cos^2(2\theta)$ for Raman measurements in crossed (XY) polarization, as $\sin^2(2\theta)$ for Raman measurements in parallel (XX) polarization, where θ is the angle between the crystallographic axis and the electric field direction (X) of the incident light. We have checked that the peak at ~370 cm^{-1} obeys the same polarization selection rules of the Ge–Ge peak at ~300 cm^{-1}. Hence, because the local symmetry is preserved, this definitively proves that the peak at ~370 cm^{-1} is directly related to the substitutional Al atoms.

In the visible region, germanium has an optical absorption much higher than silicon. The optical penetration depth (i.e., the length in which the intensity of the light is reduced by a factor $1/e$) depends on the wavelength and, in correspondence of our excitation laser lines (i.e., 514.5 nm, 568.2 nm and 647.1 nm) is about 17 nm, 25 nm and 80 nm (indicated with vertical lines in Fig. 1) [13]. As a consequence, we can probe the implanted samples with regard to Al distribution at different depths, simply by using different excitation laser lines of different wavelengths.

Let us indicate with $L(\lambda)$ the optical penetration depth at the wavelength λ. Owing to the optical absorption, the intensity of the Raman signal due to Al–Ge bonds at the depth x, from the sample surface, will be proportional to ~$e^{-2x/L(\lambda)}$. Therefore, for a given sample measured at the wavelength λ, the intensity of the Al–Ge Raman peak is proportional to

$$\int_0^{+\infty} P(x)e^{-2x/L(\lambda)}dx \qquad (3)$$

where $P(x)$ is the distribution of the substitutional Al atoms as a function of the depth x.

For each sample and laser wavelength, we have calculated the integral above using, as $P(x)$ distribution, the SRP profiles displayed in Fig. 1; the values for $L(\lambda)$ were calculated by Ref [13]. Fig. 3 shows the relative intensity of the Al–Ge Raman peak (i.e., the area of the Al–Ge peak normalized to the area of the Ge–Ge peak) plotted against the calculated values for the integral 3. As it can be observed, there is a linear relationship between intensity of the Al–Ge peak and the integral 3. If the same procedure is repeated using, as $P(x)$, the SIMS profiles displayed in Fig. 1, no similar trend is observed. As a result, we can conclude that the electrically active content of our Al-implanted Ge samples is entirely due to the substitutional Al atoms and other possible

contributions, given for example by the presence of defects [14], are negligible.

Before the conclusions, the Ge–Ge Raman peak at ~300 cm^{-1} deserves some additional considerations. Depending on the Al doping and laser wavelength, the mean position of the Ge–Ge peak shifts towards lower frequencies with respect to the pure Ge: about $-3 \div -5$ cm^{-1} for the sample annealed at 400 °C, about $-0.5 \div -1.5$ cm^{-1} for the sample annealed at 400 °C + 700 °C. The Raman peak shift can be due to strain, phonon confinement or carrier concentration effects. Since the existence of nanocrystalline regions or clusters was excluded by Transmission Electron Microscope investigations [10], the presence of phonon confinement effects can be disregarded. Moreover, the lattice strain in implanted and annealed samples typically does not exceed some 0.1%, also for high doping level [15,16]. This corresponds, according to Peng et al. [17], to a Raman peak shift of only a few 0.1 cm^{-1}. According to Cerdeira-Cardona [18] and to a more recent work of O'Reilly et al. [19], a major effect on the Raman peak position is expected in the case of high doping level achieved. As a result, we can infer that the reduction in the Raman Ge–Ge peak shift observed with the increase of the annealing temperature, is directly related to the electrical deactivation of dopant atoms observed by spreading resistance measurements.

4. Conclusions

In this work, Ge samples implanted with Al and annealed have been investigated by micro-Raman spectroscopy using different excitation lines, with the aim of studying the Al distribution at different depths.

The Raman peak observed at about 370 cm^{-1} has been attributed to the local vibrational mode of the substitutional Al atoms. By exploiting the different optical penetration depths, the intensity of the Al–Ge Raman peak at ~370 cm^{-1} has been directly correlated with the SRP measurements. No similar correlation is observed between Al–Ge Raman peak and SIMS profiles and, therefore, we can conclude that only the substitutional Al atoms contribute to the electrically active content.

Finally, we have observed a negative shift of the Ge–Ge Raman peak at ~300 cm^{-1}, which is also related to the electrically active content of Al dopant atoms. This work shows that micro-Raman spectroscopy offers interesting perspectives for the study of doping profiles in Ge.

Fig. 3. Linear relationship between the intensity of the Al–Ge Raman peak at ~370 cm^{-1} and the electrically active content of Al, probed by Raman, estimated by the Spreading Resistance Profiles (see text). Circles and triangles refer to the samples annealed at 400 °C and 400 °C + 700 °C, respectively. Full, open and cross symbols refer to the excitation laser lines 647.1 nm, 568.2 nm and 514.5 nm, respectively.

References

[1] J. Vanhellemont, E. Simoen, J. Electrochem. Soc. 154 (2007) H572.
[2] C. Claeys, E. Simoen, Germanium-Based Technologies — From Materials to Devices, Elsevier, Amsterdam, 2007.
[3] H. Kim, C.O. Chui, K. Saraswat, P.C. McIntyre, Appl. Phys. Lett. 83 (2003) 2647.
[4] H. Shang, H. Okorn-Schimdt, J. Ott, P. Kozlowski, S. Steen, E.C. Jones, H.S.P. Wong, W. Hanesch, IEEE Electron Device Lett. 24 (2003) 242.
[5] G. Impellizzeri, S. Mirabella, E. Bruno, A.M. Piro, M.G. Grimaldi, J. Appl. Phys. 105 (2009) 063533, (105).
[6] G. Impellizzeri, S. Mirabella, A. Irrera, M.G. Grimaldi, E. Napolitani, J. Appl. Phys. 106 (2009) 013518.
[7] V.I. Fistul, in: Impurities in Semiconductors: Solubility, Migration, and Interactions, CRC Press, Boca Raton, FL, 2004, p. 157.
[8] T. Itoh, I. Ohdomari, Jpn. J. Appl. Phys. 10 (1971) 1002.
[9] P. Dorner, W. Gust, A. Lodding, H. Odelius, B. Predel, U. Roll, Acta Metall. 30 (1982) 941.
[10] G. Impellizzeri, E. Napolitani, S. Boninelli, V. Privitera, T. Clarysse, W. Vandervorst, F. Priolo, Appl. Phys. Express 5 (2012) 021301.
[11] G. Contreras, M. Cardona, A. Compaan, Solid State Commun. 53 (1985) 857.
[12] M.A. Renucci, J.B. Renucci, M. Cardona, in: Balkanski (Ed.), Flammarion, Paris, 1971, p. 326.
[13] D.E. Aspnes, A.A. Studna, Phys. Rev. B 27 (1983) 985.
[14] K.S. Jones, E.E. Haller, J. Appl. Phys. 61 (1987) 2469.
[15] G. Bisognin, S. Vangelista, M. Berti, G. Impellizzeri, M.G. Grimaldi, J. Appl. Phys. 107 (2010) 103512.
[16] E. Bruno, G.G. Scapellato, G. Bisognin, E. Carria, L. Romano, A. Carnera, F. Priolo, J. Appl. Phys. 108 (2010) 124902.
[17] C.Y. Peng, C.F. Huang, Y.C. Fu, Y.H. Yang, C.Y. Lai, S.T. Chang, C.W. Liu, J. Appl. Phys. 105 (2009) 083537.
[18] F. Cerdeira, M. Cardona, Phys. Rev. B 5 (1972) 1440.
[19] L. O'Reilly, K. Horan, P.J. McNally, N.S. Bennett, N.E.B. Cowern, A. Lankinen, B.J. Sealy, R.M. Gwilliam, T.C.Q. Noakes, P. Bailey, 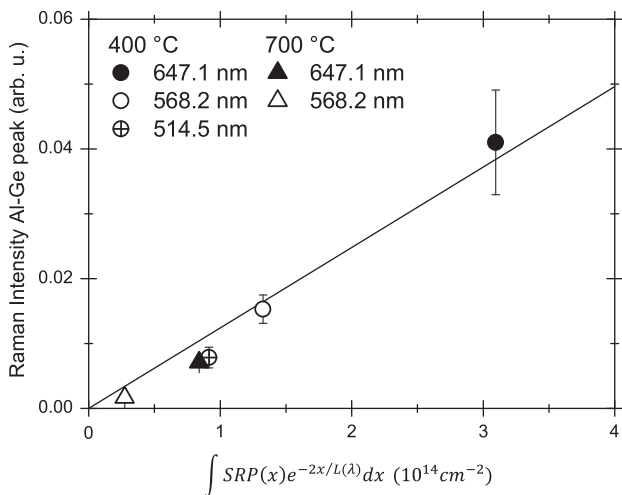Appl. Phys. Lett. 92 (2008) 233506.